Orientation in large-area semiconducting 2-amino-anthracene thin films fabricated by dynamic floating film transfer method

Atul Sankhar Mani Tripathi, Kirill Kondratenko, Benoît Duponchel, N. Hurduc, I. Carlescu, Yahia Boussoualem, Abdelylah Daoudi

Orientation in large-area semiconducting 2-amino-anthracene thin films fabricated by dynamic floating film transfer method

A. S. M. Tripathi[1*], K. Kondratenko[1], B. Duponchel[1], N. Hurduc[2], I. Carlescu[2], Y. Boussoualem[1], and A. Daoudi[1]

[1]Unité de Dynamique et Structure des Matériaux Moléculaires, EA4476.Université du Littoral Côte d'Opale, 59140, Dunkerque, France.

[2]Department of Natural and Synthetic Polymers, "Cristofor Simionescu" Faculty of Chemical Engineering and Environmental Protection, "Gheorghe Asachi" Technical University of Iasi, 700050 Iasi, Romania

*email: atul.tripathi@univ-littoral.fr

Abstract

In organic electronics, fabrication of stable, soluble, and uniform thin films of large surface area is highly important for a wide range of organic device applications. However, these objectives are difficult to achieve when using organic liquid crystalline molecules. This work focuses on a molecular organic material synthesized in our lab which was used to fabricate large-area thin films by applying the recently developed ribbon-shaped floating film transfer method (FTM). After establishing the most optimal casting parameters, organic molecule thin films of large surface area (up to 15 cm in length and 2 cm in width) were obtained. Subsequent polarized optical microscopy and atomic force microscopy investigations confirmed that film morphology and texture was uniform. Further, UV spectroscopy measurements using a polarizer were performed to study the π-π conjugation, indicating that the films exhibited optical anisotropy, as a Dichroic Ratio (DR) of 3.8 was obtained, with a 10 nm redshift in parallel FTM relative to the spin-coating method.

Keywords: Organic semiconductor, Molecular orientation, Floating film transfer method, Polarized absorption, Liquid crystal.

1. Introduction

Due to the widespread application of organic field-effect transistors (OFETs) in integrated circuits, active matrix and flexible displays, as well as sensors, organic semiconductors are gradually replacing conventional inorganic semiconductor materials [1, 2]. OFETs exhibit many advantages over conventional Si-based thin-film transistors, including facile modification at the molecular level, low fabrication cost, ease of fabrication, and flexibility [3, 4]. Consequently, ample body of research has been dedicated to improving the charge carrier mobility and stability of organic materials, as well as optimizing specific device performance characteristics [5, 6]. Currently, many types of organic semiconducting molecules are incorporated into the active semiconductor layer in the OFET channel by a simple solution processing method with many advantages over polymers [7−9], as a well-defined structure of high purity can be attained by the sublimation method. In particular, pentacene has been shown to exhibit excellent mobility (> 1cm^2/Vs), as well as good solubility in some common solvents [10, 11]. Similarly, anthradithiophene, tetracene, and dithiotetrathiafulvalene have been reported to possess superior transistor characteristics [12, 13]. According to the available findings, oxidative stability of anthracene-based semiconductors is higher than that of those based on pentacene [14]. Specifically, Ito and colleagues established that, in linear acenes, increasing the number of benzene molecules decreases oxidative stability due to the increase in the

highest occupied molecular orbital energy level [15]. Moreover, Park et al. demonstrated that triisopropylsilylethynyl anthracene derivative exhibited high solubility and moderate performance when incorporated into OFETs by solution processing method [16]. As strong π-π overlap is important for enhancing the transfer integral and charge hopping (and thus charge transport), these aspects in anthracene-based liquid crystalline molecules possessing semiconducting properties were investigated by Mery et al. [17] focusing on 2, 6 substituted derivatives, and Chen et al. who explored 2-substituted derivatives based on anthracene [18]. Recently, our group design an (E)-N-(anthracen-2-yl)-1-(4-(decyloxy)-phenyl) methanimine (10-OPIA) molecule exhibiting mesogenic properties [19], as shown in Figure 1. These molecules can be easily prepared from available substances and possess excellent solubility in various organic solvents. As indicated in our original work, 10-OPIA exhibits interesting photoconductive properties [19], making it a good candidate for a wide range of photosensitive devices. As a part of our investigation, these materials were utilized to fabricate thin solid films which were successfully transferred to appropriate substrates. As controlling the thin film morphology is also important for high-performance organic device applications, several methods can be used to fabricate thin films by solution-processed methods, such as mechanical rubbing [20], friction transfer method [21], solution sharing [22], capillary action [23], doctor blading [24], and dip coating [25]. However, all these approaches suffer from some notable drawbacks, including high material wastage, high cost, need for advanced instruments, insufficient film uniformity, and potential damage to the material structure during the multilayer

casting process. Most importantly, the shear force used in these methods typically results in face-on orientation, which is unsuitable for planar devices like OFETs. In contrast, thin film deposition by slow solvent evaporation thermodynamically favors edge-on orientation making it suitable for planar devices [26, 27]. These benefits are achieved by the recently developed dynamic floating film transfer method (FTM) [28, 29], which necessitated designing a custom-made assisting slider, allowing the film to spread in a single direction [30]. The slider not only overcomes the drawbacks of the conventional FTM, but it also assists in the formation of large-area rectangular thin films, due to which this process is denoted as ribbon-shaped FTM [31]. Thus far, this method has been applied to several conjugated polymers of different structures [32−34] with the goal of employing them in photovoltaic applications, light-emitting devices, or in high charge transport. The newly developed FTM can easily be applied to these polymers to obtain oriented thin films of at least 20 cm length and 2 cm width. As the casting conditions depend on the nature of the polymer, the resulting FTM-based films are more suitable for planar devices like OFET, as the edge-on orientation promotes charge transfer from the source to the drain electrode. Moreover, Pandey and colleagues have shown that this method is suitable for oriented composite films comprising of 2D materials dispersed within the polymer matrix, which enhances the charge carrier mobility [35]. Recently, FTM was shown to lead to better device performance compared to other deposition techniques when used in sensing applications [36, 37]. Despite these advances, further research into the FTM

application to organic molecules is needed to further improve the thin film morphology for OFET applications.

In the present study, we focused on controlling the thin film morphology of an organic material (10-OPIA) obtained by applying the recently developed ribbon-shaped dynamic FTM process combined with the spin-coating method. Our findings revealed that a uniform 10-OPIA thin film can be successfully obtained on a liquid substrate even in large-scale production with minimal material wastage and resource utilization, as uniform transfer on the substrate can be achieved by stamping. Thus, 10-OPIA as well as other molecular liquid crystalline organic materials fabricated by ribbon-shaped FTM can be used in semiconductor manufacturing.

2. Experimental Methods:

In the present study, the 10-OPIA semiconducting properties were investigated, as organic molecules having photoreactive properties are highly beneficial in a wide range of applications. As previously demonstrated by Kondratenko et al., in these molecules, the phenyl moiety is derived from to the anthracene by imine linkage, and is further enhanced by simple nucleophilic addition between 2-aminoanthracene and para-benzaldehyde derivatives [19]. The alkyl spacer can be precisely controlled by adopting an appropriate alkyl halide precursor. Figure 1 shows the chemical structure of 10-OPIA. For thin film fabrication, an organic molecule solution was prepared in dehydrated chloroform (purchased from Sigma Aldrich) followed by stirring on a hotplate for 60 minutes at 50 ^{o}C. Next, 15 µl of the molecule solution was poured in

the center of the assisting slider placed at one edge of a rectangular tray and partially filled with liquid substrate.

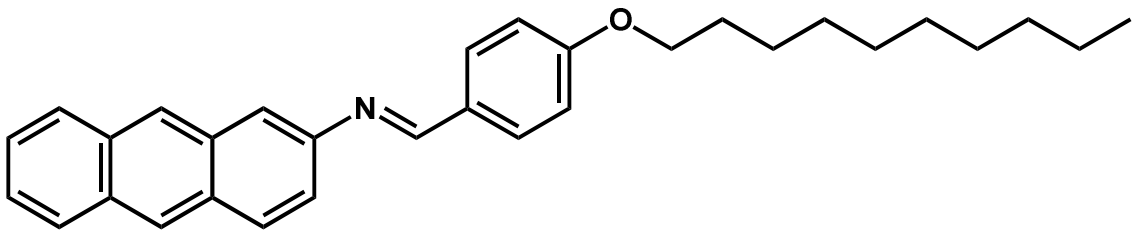

Figure 1: Chemical structure of (E)-N-(anthracen-2-yl)-1-(4-(decyloxy)-phenyl) methanimine (10-OPIA)

As a result of stirring, the molecule solution spreads in a single direction and forms a solid floating film on the liquid substrate. For the most optimal casting results, the conditions were optimized by adopting a suitable binary mixture of viscous liquid substrates, in this case ethylene glycol (EG) and glycerol (GL), adjusting the casting temperature (of both molecule solution and the viscous liquid substrate) to 30−60 ^{o}C, and varying the concentration of molecules in the chloroform solvent in the 0.5−4% w/w range. In the present study, the optimized casting conditions involved mixing EG and GL at a 3:1 ratio to form a viscous liquid substrate, applying 3% w/w molecule concentration, and setting the casting temperature to 40 ^{o}C. The resulting FTM-prepared oriented films were transferred on a pre-cleaned glass substrate by stamping. For comparison, films were also prepared by spin coating, for which 1% w/w molecule solution was prepared in chloroform solvent and was spun for 60 s at 1000 rpm, after which isotropic films were deposited by spinning the solution at 1000 rpm.

For all calorimetric investigations conducted as a part of this work, TA Instruments Q1000 Differential Scanning Calorimeter (DSC) was utilized while varying the

temperature from -180 ^{o}C to 725 ^{o}C. In addition, polarized optical microscopy (POM) was conducted using Olympus BX60F5 alongside Linkam LTS 350 hot stage (at temperatures in the -196−350 ^{o}C range), and Linkam TMS 93 controller was used for texture characterization and quantification of material changes. UV-Visible spectrophotometer Varian (Agilent) Cary 100 and Perkin Elmer Lambda 2 spectrometers equipped with Thomson polarizer were also employed for capturing the polarized absorption spectrum. Finally, all atomic force microscope (AFM) images presented here were obtained with the help of Veeco (Bruker) Multimode III in tapping mode.

3. Results and Discussion:

3.1 Thermophysical and mesogenic properties

The phase behavior of 10-OPIA molecules was investigated via calorimetric analysis conducted using DSC. The results obtained during both heating and cooling cycles are shown in Figure 2. As can be seen from the DSC thermograms, 10-OPIA exhibits mesomorphic properties since it displays at least four phase transitions, which are reversible, as they are observed in the heating as well as cooling cycle.

To gain further insight into these phase transitions, we commenced with heating, which led to the first transition and the emergence of two splitting peaks at 139 ^{o}C resulting from melting from the crystalline phase to a first smetic mesophase, denoted as Sm_1. Further, at 145 ^{o}C, a second phase transition occurs with relatively small enthalpy changes that show a slight reduction in order and suggest a second smetic mesophase, labeled Sm_2. The next phase transition occurred at 152 ^{o}C with two similar

peaks, but more significant enthalpy changes. The high energy changes observed at this transition indicate a consequential order loss from Sm_2 to a nematic (N) phase. At the last stage of heating, at 160 ^oC, complete melting occurs from the N phase to a completely disordered isotropic liquid phase (Iso).

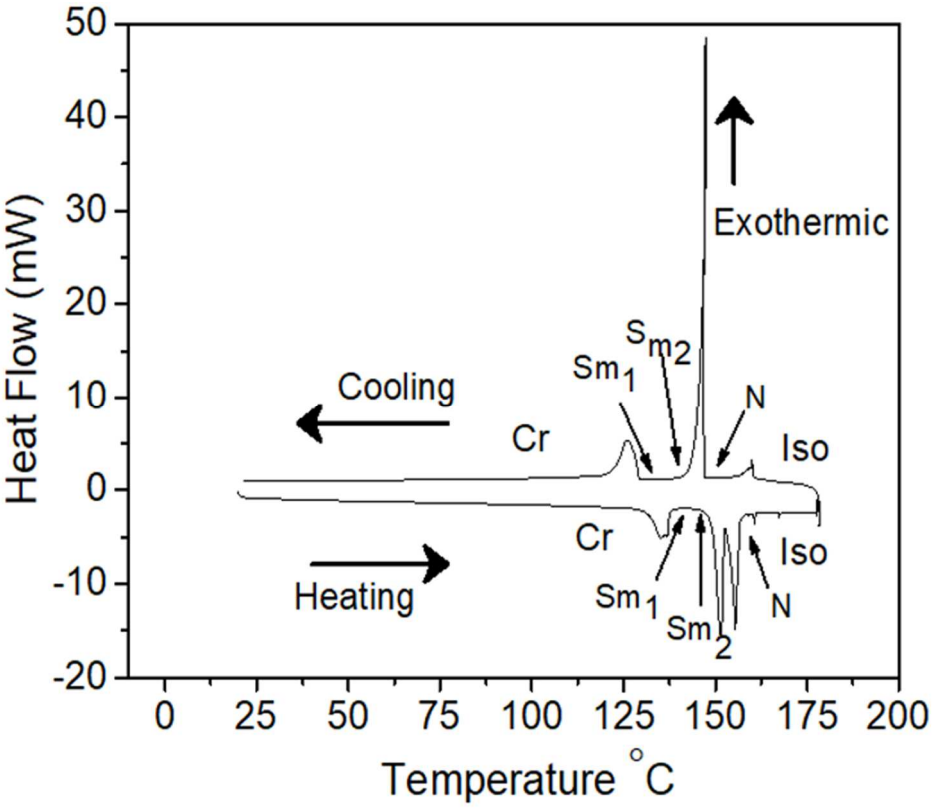

Figure 2: DSC thermograms of the heating and cooling 10-OPIA cycles at a rate of 10 ^oC/min.

The cooling cycle shows a similar phase sequence to that observed during heating, with a slight shift in the phase transition temperature towards lower values. The optical texture of the two smetic phases, Sm_1 and Sm_2, is similar to the Cr phase (Figure 3) of the polarized microphotograph of a 5 µm-thick cell with a homogenous alignment of 10-OPIA, which is supported by the findings yielded by DSC analysis. The

homogenous texture observed at 159 °C (Figure 3(d)) confirms the mesophase's nematic nature indicated by the DSC measurements.

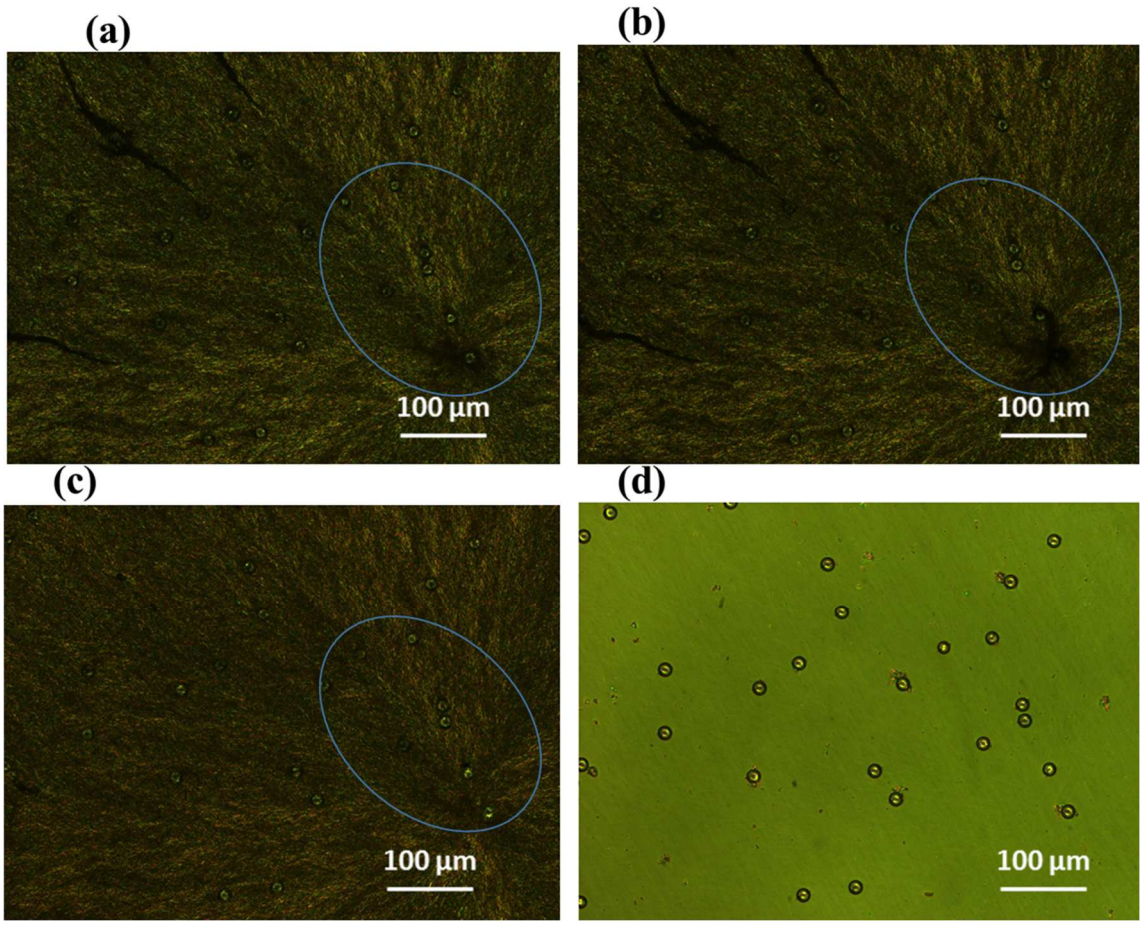

Figure 3: Texture of a 5 µm-thick 10-OPIA sample captured by POM through crossed analyzer-polarizer: (a) Crystalline (Cr) phase at 120 °C; (b, c) Sm_1 and Sm_2 mesophase at 140 °C and 148 °C, respectively; and (d) nematic mesophase at 159 °C.

3.2 Large-area thin film preparation via ribbon-shaped FTM

As thin film deposition technique is essential for high charge carrier transport, Kondratenko et al. [19] adopted the drop-casting method for this purpose and demonstrated that the resulting 10-OPIA thin films can be employed in OFET and phototransistor devices. However, the film thickness was excessive (up to 220 nm) and

non-uniform, and is thus unsuitable for high-performance applications. To overcome these issues, the recently developed ribbon-shaped FTM was utilized in this work [30]. The film orientation, thickness, and dimensions were carefully controlled by modifying the casting parameters, including the solution concentration of organic material, casting temperature (both liquid substrate and solution), liquid substrate viscosity, etc. [30, 38]. The FTM was applied to several semiconducting polymers by using the conventional and newly developed ribbon-shaped method for comparison [32, 39]. Among the various semiconducting polymers, poly(didodecyl-quaterthiophene) showed the highest dichroic ratio (DR) >20. On the other hand, poly[2,5-bis(3-tetradecylthiophen-2-yl)thieno[3,2-b]thiophene] exhibited the highest charge transport anisotropy (having mobility > 1 cm^2/Vs) [31, 40], confirming that this method is superior to other commonly applied strategies. To further test its utility, several conducting polymers and hybrid materials were fabricated via this method while controlling the casting parameters, as the optimal conditions are highly dependent on the material structure and characteristics [36]. However, this method has never been applied on highly conductive organic molecules due to their high solubility and film fragility stemming from the highly crystalline nature of the material. Consequently, in this study, liquid crystalline molecules (10-OPIA) were employed for large-area thin film fabrication on a liquid substrate by ribbon-shaped FTM, while adopting casting conditions different from those needed to obtain conjugated polymers (CPs). As has been previously shown, thin films can easily form on various CPs. In this work, we utilized 1% w/w polymer concentration on EG:GL (at a 3:1 ratio) liquid substrate and a

casting temperature in the 40–60 °C range, and achieved an oriented film of 20 cm length and 2 cm width. Further optical as well as electrical characterizations confirmed that the obtained film exhibited optical and electrical anisotropy [32]. On the other hand, under similar casting conditions, no film formation is observed when using organic molecules, as after being dropped into the assisting slider, the molecule solution is broken into small parts and is unevenly spread across the entire surface area due to the crystalline nature of the molecules. As these issues are not resolved by increasing the concentration from 1% to 2% w/w, these findings confirm that, to ensure that ribbon-shaped thin films are obtained, it is necessary to achieve an appropriate balance between the viscous force and solution spreading, as well as adopt the optimal casting temperature and molecule solution concentration.

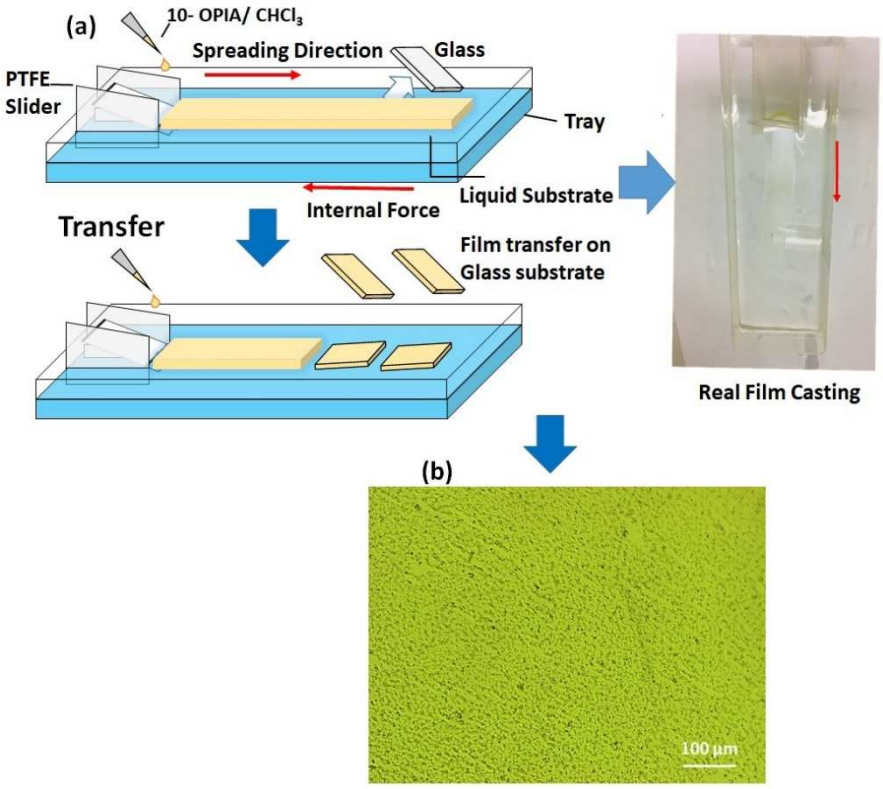

Figure 4: Thin film preparation process at optimized conditions involving EG:Gl (at a 3:1 ratio) liquid substrate, 3% w/w concentration, and 40 ^{o}C casting temperature. (a) Schematic representation and the actual film casting process comprising the ribbon-shaped floating film transfer method. (b) Optical micrograph of a film transferred on a soda-lime glass substrate.

Applying the aforementioned casting parameters—EG:GL (at a 3:1 ratio) as a liquid substrate, 40 ^{o}C casting temperature (molecule solution and liquid substrate), and 3% w/w molecule concentration—resulted in 10-OPIA thin films of 15 cm length and 2 cm width.

Figure 4(a) and Figure 4(b) show a simple schematic of the ribbon-shaped film fabrication method and real casting of 10-OPIA film, respectively. Further details of this method are provided in our previous manuscripts based on CPs [30, 31]. It is worth noting that this method is very similar to the Langmuir-Blodgett method, but it does not require application of an external force and an expensive setup. The FTM film employed in this study was obtained via a natural self-assembly process, whereby the films were oriented perpendicular to the solution spreading direction. During the spreading, solid films are formed on the liquid substrate due to the volatile nature of the solvent. Therefore, solid film orientation was caused by solvent evaporation and the opposite viscous force provided by the liquid substrate (such orientation is easily observed using a polarizer sheet). As indicated in Figure 4(a), films of much greater dimensions (up to 15 cm × 2 cm) can be obtained using this method, similar to a conjugated polymer. To verify their composition by optoelectronic characterization, the oriented solid films were transferred on the desired substrate by stamping. Figure

4(b) shows an optical micrograph of a solid film transferred on soda-lime glass, confirming that it uniformly covers the entire glass surface.

3.3 Phase transition in thin films obtained via ribbon-shaped FTM

To elucidate the processes facilitating the phase transition in FTM-prepared thin films, POM observations of the textural changes upon heating associated with phase transitions were performed. The results were compared to those obtained for bulk samples, with the texture of the FTM-coated 10-OPIA thin film shown in Figure 5 as an example. As can be seen from the image, the Sm_1 and Sm_2 texture is very similar to the crystalline phase. Moreover, the phase transition temperatures derived from the observed textural changes align with those yielded by DSC. In particular, the texture detected at around 158 ^{o}C exhibits the characteristics of the nematic phase and appears to be homogeneous.

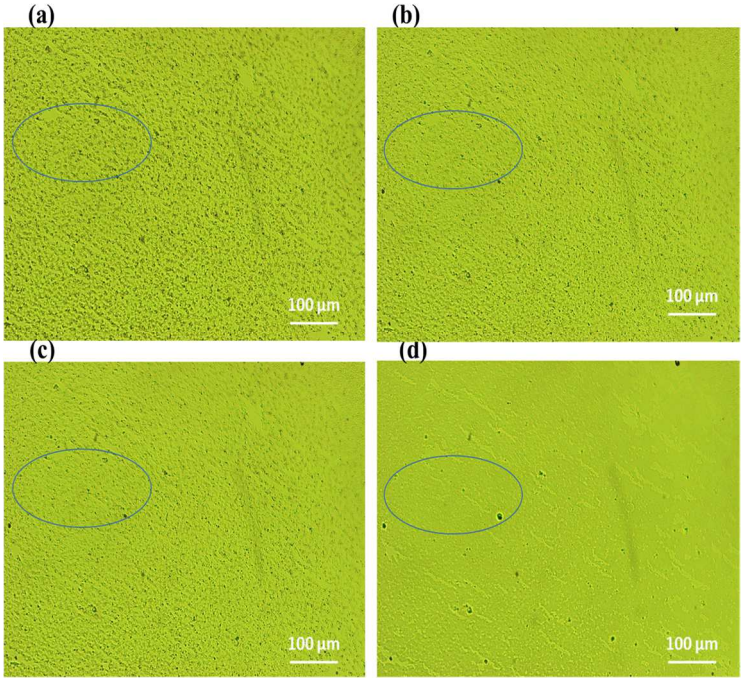

Figure 5: Texture of a FTM-processed thin-film 10-OPIA sample obtained at optimized conditions (EG:Gl-3:1 liquid substrate, 3% w/w concentration, and 40 ^{o}C casting temperature) captured by POM using a crossed analyzer-polarizer during the heating cycle: (a) Crystalline phase at 120 ^{o}C; (b, c) Sm_1 and Sm_2 mesophase at 140 and 148 ^{o}C, respectively; and (d) nematic mesophase at 158 ^{o}C.

Texture changes were also observed in the cooling cycle, as shown in Figure 6. The observed texture is much more crystalline than that obtained using the capillary method commonly applied to bulk cells. These large crystalline domains are highly desirable for OFET application because they cross the channel from the source to the drain electrode.

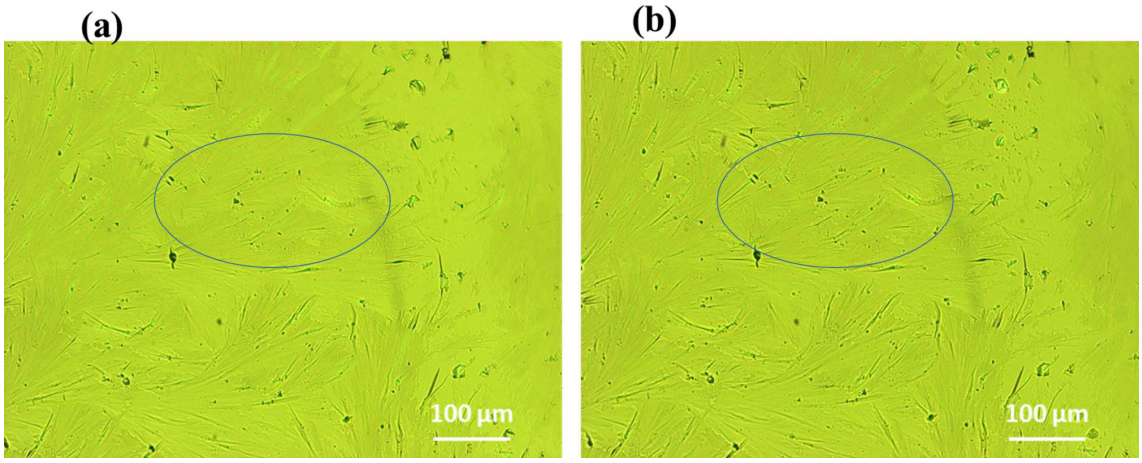

Figure 6: Texture of a FTM-processed thin-film 10-OPIA sample prepared at optimized conditions (EG:Gl-3:1 liquid substrate, 3% w/w concentration, and 40 ^{o}C casting temperature) captured by POM using a crossed analyzer-polarizer during the cooling cycle at (a) 120 ^{o}C and (b) 145 ^{o}C.

3.4 Optical characterization of 10-OPIA samples

As described above, application of the ribbon-shaped FTM leads to large-area uniform thin films of appropriate molecular orientation. To quantitatively analyze the molecular orientation of 10-OPIA samples obtained in this work, films were transferred onto a soda-lime glass substrate by stamping and were subjected to polarized electronic absorption spectral investigations.

For this purpose, their absorbance was measured using the polarizer angle of 00° and 90°, i.e., parallel and perpendicular to the molecular orientation direction.

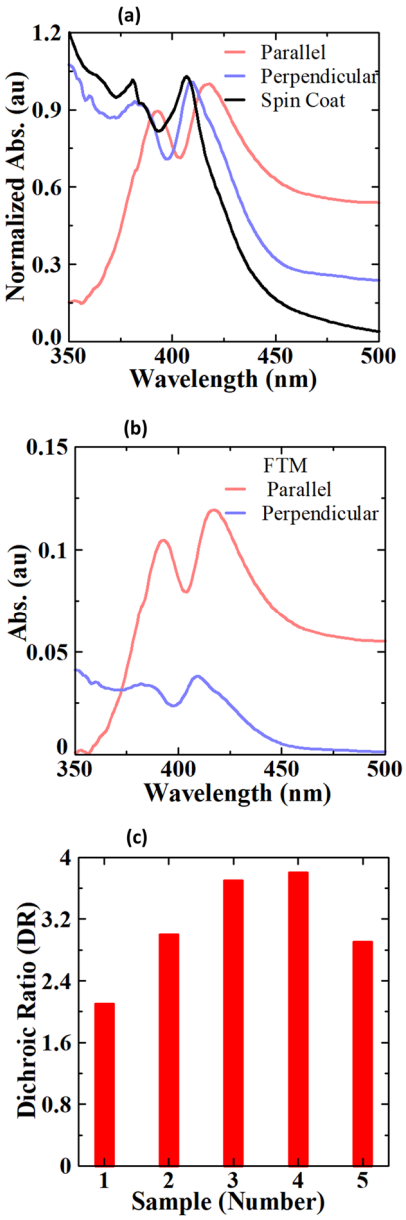

Figure 7: Optical characterization of a 10-OPIA thin film prepared at optimized conditions (EG:Gl-3:1 liquid substrate, 3% w/w concentration, and 40 °C casting temperature. (a) Normalized polarized and non-polarized electronic absorption spectra of FTM parallel, perpendicular, and spin-coated 10-OPIA thin films. (b) Polarized electronic absorption spectra of FTM-processed 10-OPIA thin films, and (c) DR values of five tested samples.

Figure 7(a) shows the normalized polarized and non-polarized electronic absorption spectra of 10-OPIA molecules, revealing obvious differences in the absorption spectra

produced by FTM parallel and perpendicular as well as spin-coated thin films. The film absorption was recorded in the 350 to 475 nm range, while λ = 360−470 nm was adopted for parallel and perpendicular measurements, and λ = 375−450 nm for spin-coated samples. In this absorption range, the maximum absorbance peak was observed at 418 nm, 409 nm, and 408 nm for parallel, perpendicular, and spin-coated samples, respectively. Although these values are comparable, a 10-nm shift between the peaks of spin-coated and parallel-orientation films is noteworthy.

Polarized electronic absorption spectra of 10-OPIA samples obtained by ribbon-shaped FTM are shown in Figure 7(b). It is evident that, when the incident beam angle relative to the film surface changes from 00^{o} to 90^{o}, optical absorption anisotropy occurs due to the molecular orientation having a DR of 3.8. To quantify the optical anisotropy of the polarized absorption spectrum of the corresponding 10-OPIA sample obtained by ribbon-shaped FTM, DR was calculated as DR = A∥/A⊥, i.e., as the ratio of maximum absorbance parallel A∥ at λmax∥ to absorbance in perpendicular, A⊥ at λmax∥. The findings for thin films prepared by the FTM and spin-coating method are reported in Table 1, confirming increased π-orbital delocalization on the molecules [36]. These results indicate that the films fabricated by this advanced method also have enhanced π-stacking and are thus suitable for use in optoelectronic devices. It is also worth noting that, in FTM-processed films, orientation intensity is small and that λ_{max} is red-shifted in 10-OPIA. As reported in our previous work, thin films cast via this process exhibit superior charge transport performance compared to the spin-coated films, even at weak DR [41].

Moreover, the orientation size up to several centimeter-scale can be achieved with only 15−20 µl of solution. Figure 7(c) shows the DR of five samples, ranging from 2.1 to 3.8, with an average of 3.1.

Table 1 : Optical parameters of 10-OPIA thin-film molecules prepared by FTM and those obtained by spin coating derived from their corresponding solid-state electronic absorption spectra.

Film Fabrication Conditions	**Absorption Maximum (nm)**	**Dichroic Ratio (DR)**
Spin Coat	408	-
FTM Parallel	418	3.8 (maximum)
FTM Perpendicular	409	-

Figure 8 provides AFM images of a spin-coated and an oriented 10-OPIA film prepared by dynamic-FTM. As shown in Figure 8(b), the spin-coated film is characterized by a

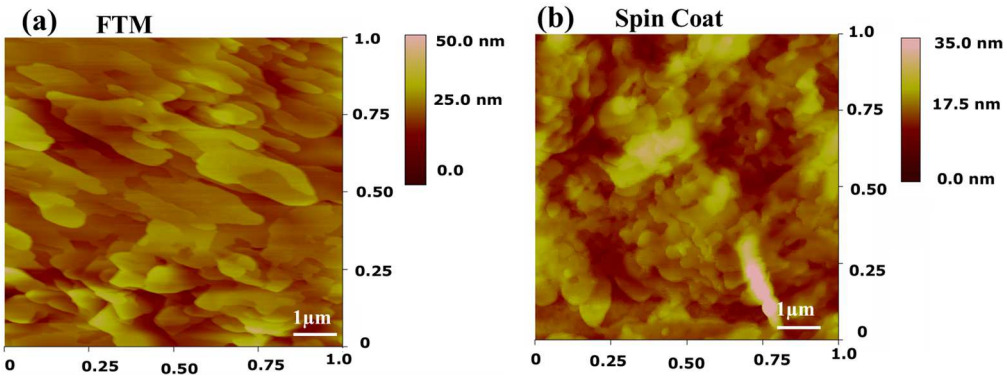

Figure 8: AFM images of a 10-OPIA thin-film sample fabricated by FTM and spin-coating method. (a) FTM at optimized conditions (EG:Gl-3:1 liquid substrate, 3% w/w concentration, and 40 ^{o}C casting temperature). (b) Spin coating at 1% w/w concentration with 1000 rpm for 60 s.

featureless surface, whereas oriented 10-OPIA film prepared by dynamic-FTM exhibits clear stretched nano-size corrugations that are aligned in the same direction over its

entire surface, as shown in Figure 8(a). The direction evident in the AFM images corresponds to that visualized optically by absorption spectroscopy.

As demonstrated in this work, ribbon-shaped FTM produces uniform films of organic crystalline-based molecular material. The obtained thin films of anthracene derivative have several advantages compared to similar materials fabricated by drop-casting in terms of uniformity, thickness, and alignment, and can be applied in a variety of devices by utilizing a few µl of molecule solution. Using this material, Kondratenko et al. obtained films of > 200 nm thickness by drop-casting with low (0.5 % w/w) concentration in chlorobenzene solvent [19]. As OFET performance depends on several factors, including processing conditions, semiconductor insulator/metal interface, and the active semiconductor layer thickness [42, 43] and pentacene material thickness affects the molecular crystal packing and grain size [44, 45], the findings reported in this work indicate that the FTM can be used for OFET applications. It is also worth noting that grain boundaries are caused by variations in morphology caused by greater film thickness, which is undesirable, as charge carriers are trapped, compromising the device performance [46, 47]. According to the available evidence, OFET mobility decreases when the active layer thickness exceeds 100 nm. These issues can be overcome by FTM [31, 32], as film uniformity and thickness can be precisely controlled, making it suitable for large-scale fabrication of organic electronics devices.

4. Conclusion:

In this work, an organic semiconducting molecular material with a film morphology controlled by a recently developed ribbon-shaped FTM was synthesized to obtain floating solid films of a large surface area (up to 15 cm × 2 cm). The findings yielded by polarized optical microscopy confirmed their optical homogeneity, as indicated by the DR of 3.8. Moreover, the absorbance spectrum produced by the parallel film exhibited 10-nm redshift compared to the spin-coated sample, indicating better π-π conjugation. Finally, when the film morphology was evaluated by AFM, a well-aligned structure of films prepared by FTM was confirmed, indicating that this method can be adopted for large-scale applications.

Acknowledgment

The authors thank ULCO, Region Hauts-de-France, for financial support for this project.

5. References:

[1] Q. Tang, Y. Tong, W. Hu, Q. Wan, T. Bjørnholm, Assembly of nanoscale organic single-crystal cross-wire circuits, Adv. Mater. 21 (2009) 4234–4237. doi:10.1002/adma.200901355.

[2] S.R. Forrest, The path to ubiquitous and low-cost organic electronic appliances on plastic, Nature. 428 (2004) 911–918. doi:10.1038/nature02498.

[3] H.R. Tseng, H. Phan, C. Luo, M. Wang, L.A. Perez, S.N. Patel, L. Ying, E.J. Kramer, T.Q. Nguyen, G.C. Bazan, A.J. Heeger, High-mobility field-effect transistors fabricated with macroscopic aligned semiconducting polymers, Adv. Mater. 26 (2014) 2993–2998. doi:10.1002/adma.201305084.

[4] H. Yan, Z. Chen, Y. Zheng, C. Newman, J.R. Quinn, F. Dötz, M. Kastler, A. Facchetti, A high-mobility electron-transporting polymer for printed transistors, Nature. 457 (2009) 679–686. doi:10.1038/nature07727.

[5] Y. Yuan, G. Giri, A.L. Ayzner, A.P. Zoombelt, S.C.B. Mannsfeld, J. Chen, D. Nordlund, M.F. Toney, J. Huang, Z. Bao, Ultra-high mobility transparent organic thin film transistors grown by an off-centre spin-coating method, Nat. Commun. 5 (2014) 1–9. doi:10.1038/ncomms4005.

[6] Y. Qiu, Y. Hu, G. Dong, L. Wang, J. Xie, Y. Ma, H2O effect on the stability of organic thin-film field-effect transistors, Appl. Phys. Lett. 83 (2003) 1644–1646. doi:10.1063/1.1604193.

[7] T. Izawa, E. Miyazaki, K. Takimiya, Solution-processible organic semiconductors based on selenophene-containing heteroarenes, 2,7-dialkyl[1]benzoselenopheno[3,2-b][1]benzoselenophenes (C n-BSBSs): Syntheses, properties, molecular arrangements, and field-effect transistor characteristics, Chem. Mater. 21 (2009) 903–912. doi:10.1021/cm8030126.

[8] S. Liu, W.M. Wang, A.L. Briseno, S.C.B. Mannsfeld, Z. Bao, Controlled deposition of crystalline organic semiconductors for field-effect-transistor applications, Adv. Mater. 21 (2009) 1217–1232. doi:10.1002/adma.200802202.

[9] C.D. Sheraw, T.N. Jackson, D.L. Eaton, J.E. Anthony, Functionalized pentacene active layer organic thin-film transistors, Adv. Mater. 15 (2003) 2009–2011. doi:10.1002/adma.200305393.

[10] J.E. Anthony, D.L. Eaton, S.R. Parkin, A road map to stable, soluble, easily crystallized pentacene derivatives, Org. Lett. 4 (2002) 15–18. doi:10.1021/ol0167356.

[11] K.C. Dickey, J.E. Anthony, Y.L. Loo, Improving organic thin-film transistor performance through solvent-vapor annealing of solution-processable triethylsilylethynyl anthradithiophene, Adv. Mater. 18 (2006) 1721–1726. doi:10.1002/adma.200600188.

[12] M.M. Payne, J.H. Delcamp, S.R. Parkin, J.E. Anthony, Robust, soluble pentacene ethers, Org. Lett. 6 (2004) 1609–1612. doi:10.1021/ol049593z.

[13] M. Mas-Torrent, M. Durkut, P. Hadley, X. Ribas, C. Rovira, High Mobility of Dithiophene-Tetrathiafulvalene Single-Crystal Organic Field Effect Transistors, J. Am. Chem. Soc. 126 (2004) 984–985. doi:10.1021/ja0393933.

[14] H. Meng, F. Sun, M.B. Goldfinger, G.D. Jaycox, Z. Li, W.J. Marshall, G.S. Blackman, High-performance, stable organic thin-film field-effect transistors based on bis-5′-alkylthiophen-2′-yl-2,6-anthracene semiconductors, J. Am. Chem. Soc. 127 (2005) 2406–2407. doi:10.1021/ja043189d.

[15] K. Ito, T. Suzuki, Y. Sakamoto, D. Kubota, Y. Inoue, F. Sato, S. Tokito, Oligo(2,6-anthrylene)s: Acene–Oligomer Approach for Organic Field-Effect Transistors**, (2003) 1159–1162.

[16] J.H. Park, D.S. Chung, J.W. Park, T. Ahn, H. Kong, Y.K. Jung, J. Lee, M.H. Yi, C.E. Park, S.K. Kwon, H.K. Shim, Soluble and easily crystallized anthracene derivatives: precursors of solution-processable semiconducting molecules, Org. Lett. 9 (2007) 2573–2576. doi:10.1021/ol071135d.

[17] S. Méry, D. Haristoy, J.F. Nicoud, D. Guillon, H. Monobe, Y. Shimizu, Liquid

crystals containing a 2,6-disubstituted anthracene core - Mesomorphism, charge transport and photochemical properties, J. Mater. Chem. 13 (2003) 1622–1630. doi:10.1039/b211867j.

[18] Y. Chen, C. Li, X. Xu, M. Liu, Y. He, I. Murtaza, D. Zhang, C. Yao, Y. Wang, H. Meng, Thermal and Optical Modulation of the Carrier Mobility in OTFTs Based on an Azo-anthracene Liquid Crystal Organic Semiconductor, ACS Appl. Mater. Interfaces. 9 (2017) 7305–7314. doi:10.1021/acsami.6b13500.

[19] K. Kondratenko, I. Carlescu, P. Danjou, Y. Boussoualem, A. Simion, B. Duponchel, Novel organic semiconductor based on 2-amino- anthracene : synthesis , charge transporting and photo- conductive properties, Phys. Chem. Chem. Phys. 23 (2021), 13885-13894. https://doi.org/10.1039/D1CP01427G

[20] M. Brinkmann, L. Hartmann, L. Biniek, K. Tremel, N. Kayunkid, Orienting semiconducting pi-conjugated polymers, Macromol. Rapid Commun. 35 (2014) 9–26. doi:10.1002/marc.201300712.

[21] S. Nagamatsu, W. Takashima, K. Kaneto, Y. Yoshida, N. Tanigaki, K. Yase, K. Omote, Backbone arrangement in “friction-transferred” regioregular poly(3-alkylthiophene)s, Macromolecules. 36 (2003) 5252–5257. doi:10.1021/ma025887t.

[22] T. Higashi, N. Yamasaki, H. Utsumi, H. Yoshida, A. Fujii, M. Ozaki, Anisotropic properties of aligned π-conjugated polymer films fabricated by capillary action and their post-annealing effects, Appl. Phys. Express. 4 (2011) 3–6. doi:10.1143/APEX.4.091602.

[23] G. Giri, D.M. Delongchamp, J. Reinspach, D.A. Fischer, L.J. Richter, J. Xu, S. Benight, A. Ayzner, M. He, L. Fang, G. Xue, M.F. Toney, Z. Bao, Effect of solution shearing method on packing and disorder of organic semiconductor polymers, Chem. Mater. 27 (2015) 2350–2359. doi:10.1021/cm503780u.

[24] A. Pierre, M. Sadeghi, M.M. Payne, A. Facchetti, J.E. Anthony, A.C. Arias, All-printed flexible organic transistors enabled by surface tension-guided blade coating, Adv. Mater. 26 (2014) 5722–5727. doi:10.1002/adma.201401520.

[25] S. Wang, A. Kiersnowski, W. Pisula, K. Müllen, Microstructure evolution and device performance in solution-processed polymeric field-effect transistors: The key role of the first monolayer, J. Am. Chem. Soc. 134 (2012) 4015–4018. doi:10.1021/ja211630w.

[26] J.F. Chang, B. Sun, D.W. Breiby, M.M. Nielsen, T.I. Sölling, M. Giles, I. McCulloch, H. Sirringhaus, Enhanced Mobility of poly(3-hexylthiophene) transistors by spin-coating from high-boiling-point solvents, Chem. Mater. 16 (2004) 4772–4776. doi:10.1021/cm049617w.

[27] H. Yang, S.W. Lefevre, C.Y. Ryu, Z. Bao, Solubility-driven thin film structures of regioregular poly(3-hexyl thiophene) using volatile solvents, Appl. Phys. Lett. 90

(2007) 2005–2008. doi:10.1063/1.2734387.

[28] T. Morita, V. Singh, S. Nagamatsu, S. Oku, W. Takashima, K. Kaneto, Enhancement of transport characteristics in poly(3-hexylthiophene) films deposited with floating film transfer method, Appl. Phys. Express. 2 (2009) 1–4. doi:10.1143/APEX.2.111502.

[29] A. Dauendorffer, S. Nagamatsu, W. Takashima, K. Kaneto, Optical and transport anisotropy in poly(9,9???-dioctyl-fluorene-alt- bithiophene) films prepared by floating film transfer method, Jpn. J. Appl. Phys. 51 (2012). doi:10.1143/JJAP.51.055802.

[30] A. Tripathi, M. Pandey, S. Nagamatsu, S.S. Pandey, S. Hayase, W. Takashima, Casting Control of Floating-films into Ribbon-shape Structure by modified Dynamic FTM, J. Phys. Conf. Ser. 924 (2017) 8–14. doi:10.1088/1742-6596/924/1/012014.

[31] A.S.M. Tripathi, M. Pandey, S. Sadakata, S. Nagamatsu, W. Takashima, S. Hayase, S.S. Pandey, Anisotropic charge transport in highly oriented films of semiconducting polymer prepared by ribbon-shaped floating film, Appl. Phys. Lett. 112 (2018). doi:10.1063/1.5000566.

[32] A.S.M. Tripathi, N. Kumari, S. Nagamatsu, S. Hayase, S.S. Pandey, Facile fabrication of large area oriented conjugated polymer films by ribbon-shaped FTM and its implication on anisotropic charge transport, Org. Electron. Physics, Mater. Appl. 65 (2019) 1–7. doi:10.1016/j.orgel.2018.10.043.

[33] A.S.M. Tripathi, S. Sadakata, R.K. Gupta, S. Nagamatsu, Y. Ando, S.S. Pandey, Implication of Molecular Weight on Optical and Charge Transport Anisotropy in PQT-C12 Films Fabricated by Dynamic FTM, ACS Appl. Mater. Interfaces. 11 (2019). doi:10.1021/acsami.9b06568.

[34] A.S.M. Tripathi, R.K. Gupta, S. Sharma, S. Nagamatsu, S.S. Pandey, Molecular orientation and anisotropic charge transport in the large area thin films of regioregular Poly(3-alkylthiophenes) fabricated by ribbon-shaped FTM, Org. Electron. 81 (2020) 105687. doi:10.1016/j.orgel.2020.105687.

[35] R.K. Pandey, A.S.M. Tripathi, S.S. Pandey, R. Prakash, Optoelectrical anisotropy in graphene oxide supported polythiophene thin films fabricated by floating film transfer, Carbon N. Y. 147 (2019) 252–261. doi:10.1016/j.carbon.2019.02.086.

[36] P.K. Sahu, M. Pandey, C. Kumar, S.S. Pandey, W. Takashima, V.N. Mishra, R. Prakash, Air-stable vapor phase sensing of ammonia in sub-threshold regime of poly(2,5-bis(3-tetradecylthiophen-2yl)thieno(3,2-b)thiophene) based polymer thin-film transistor, Sensors Actuators, B Chem. 246 (2017) 243–251. doi:10.1016/j.snb.2017.02.063.

[37] K. Bhargava, V. Singh, High-sensitivity organic phototransistors prepared by floating film transfer method, Appl. Phys. Express. 9 (2016).

doi:10.7567/APEX.9.091601.

[38] M. Pandey, S.S. Pandey, S. Nagamatsu, S. Hayase, W. Takashima, Controlling Factors for Orientation of Conjugated Polymer Films in Dynamic Floating-Film Transfer Method, J. Nanosci. Nanotechnol. 17 (2017) 1915–1922. doi:doi:10.1166/jnn.2017.12816.

[39] M. Pandey, S.S. Pandey, S. Nagamatsu, S. Hayase, W. Takashima, Influence of backbone structure on orientation of conjugated polymers in the dynamic casting of thin floating-films, Thin Solid Films. 619 (2016) 125–130. doi:10.1016/j.tsf.2016.11.015.

[40] M. Pandey, A. Gowda, S. Nagamatsu, S. Kumar, W. Takashima, S. Hayase, S.S. Pandey, Rapid Formation and Macroscopic Self-Assembly of Liquid-Crystalline, High-Mobility, Semiconducting Thienothiophene, Adv. Mater. Interfaces. 5 (2018) 1–11. doi:10.1002/admi.201700875.

[41] M. Pandey, S. Nagamatsu, S.S. Pandey, S. Hayase, W. Takashima, Enhancement of carrier mobility along with anisotropic transport in non-regiocontrolled poly (3-hexylthiophene) films processed by floating film transfer method, Org. Electron. 38 (2016) 115–120. doi:10.1016/j.orgel.2016.08.003.

[42] Y. Fan, J. Liu, W. Hu, Y. Liu, L. Jiang, The effect of thickness on the optoelectronic properties of organic field-effect transistors: Towards molecular crystals at monolayer limit, J. Mater. Chem. C. 8 (2020) 13154–13168. doi:10.1039/d0tc03193c.

[43] D. Gupta, Y. Hong, Understanding the effect of semiconductor thickness on device characteristics in organic thin film transistors by way of two-dimensional simulations, Org. Electron. 11 (2010) 127–136. doi:10.1016/j.orgel.2009.10.009.

[44] T. Kakudate, N. Yoshimoto, Y. Saito, Polymorphism in pentacene thin films on Si O2 substrate, Appl. Phys. Lett. 90 (2007) 1–4. doi:10.1063/1.2709516.

[45] I.P.M. Bouchoms, W.A. Schoonveld, J. Vrijmoeth, T.M. Klapwijk, Morphology identification of the thin film phases of vacuum evaporated pentacene on SIO2 substrates, Synth. Met. 104 (1999) 175–178. doi:10.1016/S0379-6779(99)00050-8.

[46] S. Verlaak, C. Rolin, P. Heremans, Microscopic description of elementary growth processes and classification of structural defects in pentacene thin films, J. Phys. Chem. B. 111 (2007) 139–150. doi:10.1021/jp0653003.

[47] G. Horowitz, M.E. Hajlaoui, Grain size dependent mobility in polycrystalline organic field-effect transistors, Synth. Met. 122 (2001) 185–189. doi:10.1016/S0379-6779(00)01351-5.

Figure and Table Captions

Figure 1: Chemical structure of (E)-N-(anthracen-2-yl)-1-(4-(decyloxy)-phenyl) methanimine (10-OPIA)

Figure 2: DSC thermograms of the heating and cooling 10-OPIA cycles at a rate of 10 ^{o}C/min.

Figure 3: Texture of a 5 µm-thick 10-OPIA sample captured by POM through crossed analyzer-polarizer: (a) Crystalline (Cr) phase at 120 ^{o}C; (b, c) Sm_1 and Sm_2 mesophase at 140 ^{o}C and 148 ^{o}C, respectively; and (d) nematic mesophase at 159 ^{o}C.

Figure 4: Thin film preparation process at optimized conditions involving EG:Gl (at a 3:1 ratio) liquid substrate, 3% w/w concentration, and 40 ^{o}C casting temperature. (a) Schematic representation and the actual film casting process comprising the ribbon-shaped floating film transfer method. (b) Optical micrograph of a film transferred on a soda-lime glass substrate.

Figure 5: Texture of a FTM-processed thin-film 10-OPIA sample obtained at optimized conditions (EG:Gl-3:1 liquid substrate, 3% w/w concentration, and 40 ^{o}C casting temperature) captured by POM using a crossed analyzer-polarizer during the heating cycle: (a) Crystalline phase at 120 ^{o}C; (b, c) Sm_1 and Sm_2 mesophase at 140 and 148 ^{o}C, respectively; and (d) nematic mesophase at 158 ^{o}C.

Figure 6: Texture of a FTM-processed thin-film 10-OPIA sample prepared at optimized conditions (EG:Gl-3:1 liquid substrate, 3% w/w concentration, and 40 ^{o}C casting temperature) captured by POM using a crossed analyzer-polarizer during the cooling cycle at (a) 120 ^{o}C and (b) 145 ^{o}C.

Figure 7: Optical characterization of a 10-OPIA thin film prepared at optimized conditions (EG:Gl-3:1 liquid substrate, 3% w/w concentration, and 40 ^{o}C casting temperature. (a) Normalized polarized and non-polarized electronic absorption spectra of FTM parallel, perpendicular, and spin-coated 10-OPIA thin films. (b) Polarized electronic absorption spectra of FTM-processed 10-OPIA thin films, and (c) DR values of five tested samples.

Figure 8: AFM images of a 10-OPIA thin-film sample fabricated by FTM and spin-coating method. (a) FTM at optimized conditions (EG:Gl-3:1 liquid substrate, 3% w/w concentration, and 40 ^{o}C casting temperature). (b) Spin coating at 1% w/w concentration with 1000 rpm for 60 s.

Table 1 : Optical parameters of 10-OPIA thin-film molecules prepared by FTM and those obtained by spin coating derived from their corresponding solid-state electronic absorption spectra.